ISSN NO. 2320-5407

Journal homepage: http://www.journalijar.com

INTERNATIONAL JOURNAL OF ADVANCED RESEARCH

RESEARCH ARTICLE

SYNTHESIS, CHARACTERIZATION, AND BIOLOGICAL APPLICATIONS OF 4-ISOPROPYL BENZALDEHYDE SEMI AND THIOSEMI CARBAZONES AND THEIR Mn(II) AND Fe(III) METAL COMPLEXES

Rosaline Ezhilarasi J* and Jaya Santhi R

P G & Research Department of Chemistry, Auxilium College, Vellore-632006, Tamil Nadu, India

Manuscript Info

Manuscript History:

Received: 15 June 2014
Final Accepted: 29 July 2014
Published Online: August 2014

Key words:

4-isopropyl benzaldehyde; semicarbazone; metal complexes; IR; ^{1}H NMR; antimicrobial activity, antioxidant

Corresponding Author

Rosaline Ezhilarasi J

Abstract

Four complexes, $[Mn(L_1)_2Cl_2]$ (1), $[Fe(L_1)_2Cl_2)]$ (2), $[Mn(L_2)_2Cl_2]$ (3), $[Fe(L_2)_2Cl_2)]$ (4), were prepared by reacting 4-isopropyl benzaldehyde semicarbazone and thiosemicarbazone ligands with $MnCl_2.4H_2O$ and $FeCl_3.6H_2O$. The infrared, UV, ^{1}H NMR, ^{13}CNMR, EPR and mass spectra of the complexes have been assigned. Thermogravimetric analyses (TGA, DTA) were also carried out. The data agree quite well with the proposed structures and show that the complexes were finally decomposed to the corresponding ligands. The ligands and their metal complexes were screened for antimicrobial activities by the disc diffusion technique using DMSO as solvent. The minimum inhibitory concentration (MIC) values for 1–4 were calculated at 30°C for 24–48 h. The activity data show that the thiosemicarbazone metal complexes are more potent antibacterials than the semicarbazone metal complexes. The complexes were also screened for their anti oxidant properties, which are comparatively lesser for manganese complexes than for iron complexes.

.

Introduction

Semicarbazones are derivatives of imines formed by condensation reaction between ketones or aldehydes and semicarbazide. They are classified as imine derivatives because they are formed from the reaction of an aldehyde or ketone with the terminal $-NH_2$ group of semicarbazide, which behaves very similarly to primary amines. Many semicarbazones are crystalline solids, useful for the identification of the parent aldehydes / ketones by melting point analysis [1]. Semicarbazones and thiosemicarbazones present a wide range of bioactivities, and their chemistry and pharmacological applications have been extensively investigated. The literature contains reviews on many aspects of the chemistry of these interesting compounds, such as preparative methods, stereochemistry, bonding in metal complexes, spectral characteristics and crystal structures [2-6].

Schiff base metal complexes have also been widely studied because of their industrial, antifungal and biological applications [7–12]. Some semicarbazones, such as nitrofurazone, and thiosemicarbazones are known to have anti-viral and anti-cancer activity, usually mediated through binding to copper or iron in cells. The biological properties of semicarbazones and thiosemicarbazones are often related to metal ion coordination. Firstly, lipophilicity, which controls the rate of entry into the cell, is modified by coordination [13]. Also, the metal complex can be more active than the free ligand, and some side effects may decrease upon complexation. In addition, the complex can exhibit bioactivities which are not shown by the free ligand. The mechanism of action can involve binding to a metal *in vivo*

or the metal complex may be a vehicle for activation of the ligand as the cytotoxic agent. Moreover, coordination may lead to significant reduction of drug-resistance [5].

2. EXPERIMENTAL

2.1. Materials and spectral measurements

All chemicals used were of analar grade. The Infrared spectra of complexes were recorded on a Bruker-Tensor 27 FT-IR spectrophotometer using KBr pellets in the range of 4000-400 cm^{-1}. Electronic spectra of the complexes were recorded in DMSO on Perkin-Elmer spectrophotometer in the range of 800-200 nm. The ^{1}H NMR spectra were recorded in DMSO-d_6 with JEOL 400 MHz instrument using TMS as internal reference. ^{13}CNMR spectra were recorded using Wedeline NMR spectrophotometer**.** EPR spectra were recorded on a Varian model E112 EPR spectrometer. Mass spectra were recorded on JEOL GC mate mass spectrometer. Thermal analyses (TGA, DTA) were carried out using a Shimadzu TGA Q50 V20.5 Build 30 computerized thermal analysis system. The system includes a program which processes data from the thermal analyzer with the ChromotPac C-R3A. The rate of heating of the samples was kept at $10^{0}C$ min^{-1}. Alumina powder was used as DTA standard material.

2.2 Synthesis of metal complexes

A solution (0.002mol; 200mL MeOH) of the respective ligand (4-isopropyl benzaldehyde semicarbazone / thiosemicarbazone) was added to the solution of (0.002mol; 20 mL H_2O) of manganous chloride, $MnCl_2.4H_2O$ and the reaction mixtures were refluxed for 3h.

A solution (0.002mol; 200mL MeOH) of the respective ligand (4-isopropyl benzaldehyde semicarbazone / thiosemicarbazone) was added to the solution of (0.002mol; 20 mL H_2O) of Ferric chloride, $FeCl_3.6H_2O$. A pinch of sodium acetate was added and the reaction mixtures were refluxed for 3h.

The obtained precipitates were removed by filtration, washed several times with water, MeOH and recrystallized from EtOH. Finally, all the obtained complexes were dried under vacuum over P_4O_{10}.

$[Mn(L_1)_2Cl_2]$ (1): Yield: 222.0 mg (89%). Color: white. Anal. Found 536.5(Calcd for $C_{18}H_{22}N_6O_6MnCl_2$, 536.5): C, 65.11 (66.54); H, 6.98 (7.02); N, 19.09 (19.15); Co, 7.86 (7.29)

$[Fe(L_1)_2Cl_2]$ (2): Yield: 185.0 mg (85%). Color: dirty white. Anal. Found 540 (Calcd for $C_{18}H_{22}N_6O_6FeCl_2$, 537): C, 60.96 (61.08); H, 6.31(6.54); N, 19.40 (19.76); Fe, 12.27 (12.62)

$[Mn(L_2)_2Cl_2]$ (3): Yield: 177.5 mg (77%). Color: white. Anal. Found 570 (Calcd for $C_{18}H_{22}N_6O_4S_2MnCl_2$, 568.5): C, 54.58 (54.97); H, 6.40 (6.26); N, 18.60 (18.75); S, 12.88 (13.44); Mn, 7.54 (6.58)

$[Fe(L_2)_2Cl_2]$ (4): Yield: 235 mg (88%). Color: grey. Anal. Found 571 (Calcd for $C_{18}H_{22}N_6O_4S_2$ $FeCl_2$, 569): C, 54.42 (54.32); H, 6.26 (6.23); N, 17.84 (18.31); S, 14.57 (14.32); Fe, 6.91 (6.82)

2.3. Antibacterial activity

The ligands and corresponding complexes were evaluated for their in-vitro antibacterial activity against five gram positive bacteria such as *Staphylococcus aureus* MTCC 96, *Micrococcus luteus* MTCC 106, *Bacillus subtilis* MTCC 10619, *Bacillus cereus* MTCC 1272, *Lactobacillus* MTCC 2997 and seven gram negative bacteria such as *Salmonella typhi* MTCC 733, *Shigella flexneri* MTCC 1457, *Pseudomonas Aeruginosa* MTCC 424, *Klebsiella Pneumoniae* MTCC 7162, *Escherichia coli* MTCC 443, *Proteus vulgaris* MTCC 1771, *Proteus mirabilis* MTCC by the disc diffusion method. Bacteria inoculums were prepared by growing cells in Mueller Hinton Broth for 24 h at $37^{o}C$. These cell suspensions were diluted with sterile MHB to provide initial cell counts of about 10^{-4} CFU/ml. The studied bacteria were incubated into Nutrient Broth for 24 h. After incubation period the culture was diluted. In this method, Petri plates were prepared with 20 ml of sterile Agar. The test cultures (100µl of suspension containing 10^{8} CFU/ml bacteria) were swabbed on the top of the solidified media and allowed to dry for 10 min. The tests were conducted at 1000 µg/disc concentration of the compounds. The loaded discs were placed on the surface of the medium and left for 30 min at room temperature for compound diffusion. Negative control was prepared using DMSO. Streptomycin (25µg /disc) was used as positive control. The plates were incubated at $37^{o}C$ for 24 hours. Zone of inhibition was recorded in millimeters and the antibacterial tests were calculated as a mean of three replicates and the SD was calculated using the software SPSS.

2.4. Determination of minimal inhibitory concentration (MIC)

Nutrient agar is employed as basal medium for the growth of bacteria, during the test of 1, 2, 3 and 4. The culture medium (20 mL) was poured into Petri dishes (9mm in diameter) and maintained at $37^{0}C$ until the samples were incorporated into the agar. The samples were added as 1mL using an automatic micropipette while constantly

stirring to assure a uniform distribution. Each sample was tested at 25, 50, 75, 100, 125, 150, 175, and 200 mmol mL^{-1} in DMSO. The different bacterial strains were layered to place 30 mL over the surface of the solidified culture medium containing a sample. After the bacteria were absorbed into the agar, the plates were incubated at 30^0C for 24–48 h. Bacterial growth was monitored visually and the MIC was determined [20, 22].

2.5. Antioxidant activity:

The antioxidant activity was measured by the method of Mensor *et al* (2001). Different concentration of each sample (5, 10, 20, 40, 60, 80, 100µg/ml) were prepared. To each of this solution 1 ml of methanolic solution of DPPH was added, and then the tubes were made up to 3ml using methanol. The tubes were incubated at room temperature for 30 min. After 30 min of incubation, the decolourisation of the purple colour was measured at 518nm using UV spectrophotometer. The antioxidant activity was measured using the formula,

$$\% \text{ of Scavenging} = \frac{A_0 - A_S}{A_0} \times 100$$

A0 = Absorption of DPPH solution without the sample

As = Absorption of DPPH solution with the sample

3. RESULTS AND DISCUSSION

3.1. Synthesis of the metal complexes

Metal complexes 1–4 were obtained during the reaction of Manganous chloride, $MnCl_2.4H_2O$ / Ferric chloride, $FeCl_3.6H_2O$ with 4-isopropyl benzaldehyde semicarbazone / thiosemicarbazone ($L_1$and L_2). The numerical data of the physical measurements & CHN Elemental analysis data (in %) of L^1, L^2 and their metal complexes are given in Table 1. The complexes were obtained in good yields (75–89%). The structures of complexes were verified by elemental analyses, spectroscopic methods, and confirmed by thermal analysis (TGA, DTA). The metal complexes are in 1:2 stoichiometry.

3.2. Vibrational spectra

The most characteristic IR bands of the ligands (L_1 and L_2) and their metal complexes (1-4) are summarized in Table 1. The ligand L_1 shows sharp absorption band at 1686 cm^{-1} corresponding to >C=O frequency, and the presence of band in the region 1646-1686 cm^{-1} supports the keto form of the ligand in the metal complexes. Similarly, the ligand L_2 shows a sharp absorption band at 1598 cm^{-1} corresponding to >C=S frequency, and the presence of band in the region 1590-1600 cm^{-1} supports the existence of >C=S stretching in the metal complexes. A sharp band at 1601 cm^{-1} corresponds to >C=N stretching frequency for L_1 and 1590 cm^{-1} for L_2. On coordination of the azomethine nitrogen, the IR stretching frequency of >C=N shows a shift and is observed in the region 1594-1600 cm^{-1} in 1 and 2 and 1584-1591 cm^{-1} in 3 and 4. The strong bands at 3459 cm^{-1} and 3408 cm^{-1} in the spectra have been assigned to $-NH_2$ cm^{-1}. The bands at 3192 cm^{-1} and 3154 cm^{-1} in ligands are due to NH vibration. In all the complexes, the presence of a band in this region corresponds to NH vibration which indicates that the ligand is coordinated in the neutral form. In the case of metal complexes, the appearance of bands in the region of 524-554 cm^{-1} and 553-620 cm^{-1} correspond to the M-N and M-O vibrational frequencies respectively. The appearance of the band around 1131-1283 cm^{-1} corresponds to N-N stretching frequency both in ligands and in metal complexes. Aromatic ν(C=C) value appears around 1440-1486 cm^{-1} and the aromatic ν(C-H) stretching value appears in the region 3007-3190 cm^{-1} both in ligands and metal complexes.

3.3. UV spectra

The electronic absorption spectra are often very helpful in the evaluation of results furnished by other methods of structural investigation. The electronic spectral measurements were used for assigning the stereochemistry of metal ions in the complexes based on the positions and number of d–d transition peaks. The electronic absorption spectra of the ligands and its Mn (II) and Fe (III) complexes were recorded at room temperature using DMSO as solvent. The electronic absorption spectra of the compounds exhibit band around 32,000 cm^{-1} are due to n→π* transition and are associated with the azomethine functions of the semicarbazone and thiosemicarbazone moieties and they also exhibit ring π→π* transition around 40,000 cm^{-1}. The absorptions in the ultraviolet region are assignable to transitions within the ligand orbitals and that in the visible region is propably due to charge transfer transition involving ligand and metal orbitals. The ligand L^1 shows n→ π* and π→π* transitions in the region 31,250 cm^{-1} and 40,000 cm^{-1} respectively and the ligand L^2 shows n→ π* and π→π* transition in the region 37,736 cm^{-1} and 42,373 cm^{-1} respectively. Both the complexes $[Mn(L^1)_2Cl_2]$ (1) and $[Mn(L^2)_2Cl_2]$ (3) show n→ π* transition in the region 33,826 cm^{-1} and 33,857 cm^{-1} respectively and π→ π* transition in the region 39,523 cm^{-1} and 39,453 cm^{-1} respectively. The complex $[Fe(L_1)_2Cl_2)]$ (2) shows bands in the region 39,516 cm^{-1} and 44,385 cm^{-1}, due to n→π*

transition and π→π* transition respectively. The complex $[Fe(L^2)_2Cl_2]$ (4) shows bands in the region 33,557 cm^{-1} and 46,728 cm^{-1}, due to n→ π* transition and π→π* transition respectively. The electronic absorption spectral bands for L^1, L^2 and their corresponding complexes (1-4) are given in Table 3.

3.4. EPR spectra

The g-value calculated for the complexes $[Mn(L^1)_2Cl_2]$ (1), $[Fe(L^1)_2Cl_2]$ (2), $[Mn(L^2)_2Cl_2]$ (3), $[Fe(L^2)_2Cl_2]$ (4), using EPR spectroscopy are given in Table 4. $[Mn(L^1)_2Cl_2]$ (1) (Figure 1) and $[Mn(L^2)_2Cl_2]$ (3) (Figure 3) complexes show signals with six fine splitting. The complex $[Fe(L^1)_2Cl_2]$ (2) shows hyperfine splitting (Figure 2). Since the measurements are made at room temperature the fine splitting was not observed in the EPR spectrum of the metal complex $[Fe(L^1)_2Cl_2]$ (4) (Figure 4), as the spin lattice relaxation time is shorter that makes EPR hyperfine splitting possible only at liquid nitrogen temperature.

3.5. ^{1}HNMR spectra

^{1}H NMR values (ppm) of L^1, L^2 and metal complexes (1–4) in DMSO-d6 are summarized in Table 5.

3.5.1. $[Mn(L^1)_2Cl_2]$ (1). Deuterated DMSO provided adequate solubility [27] for recording ^{1}HNMR signals of L^1, L^2 and 1,2,3,4 (table 5). The complex $[Mn(L^1)_2Cl_2]$ (1) shows signal at 3.4 δ has been assigned to – C-H proton and the signals at 3.5 δ and 3.9 δ due to NH_2 and NH protons respectively. The signal at 6.4– 7.8 δ is due to aromatic protons.

3.5.2. $[Fe(L^1)_2Cl_2)]$ (2). The complex shows signal at 3.0 δ have been assigned to –C-H proton and the signals at 2.5 δ and 3.2 δ due to NH_2 and NH protons respectively. The signal at 7-8.8 δ is due to aromatic protons.

3.5.3. $[Mn(L^2)_2Cl_2]$ (3). The complex shows signal at 3.3 δ have been assigned to –C-H proton and the signals at 3.2 δ and 3.9 δ due to NH_2 and NH protons respectively. The signal at 6.8-8.2 δ is due to aromatic protons.

3.5.4. $[Fe(L^2)_2Cl_2]$ (4). The complex shows signal at 3.0 δ have been assigned to –C-H proton and the signals at 2.5 δ and 3.3 δ due to NH_2 and NH protons respectively. The signal at 7-9 δ is due to aromatic protons.

3.6. Mass spectra

The mass spectrum of the ligand L^1 ($C_{11}H_{15}ON_3$) shows a molecular ion $[M^+]$ peak at m/z 205 amu corresponding to the species $[C_{11}H_{15}ON_3]^+$, which confirms the proposed formula. It also shows a series of peaks at 175, 161, 158, 143, 132, 115, 103, 97, 91, 86, 75, 72, 61 amu corresponding to various fragments (Figure 5).

The mass spectrum of the ligand L^2 ($C_{11}H_{15}SN_3$) shows a molecular ion $[M^+]$ peak at m/z 221 amu corresponding to the species $[C_{11}H_{15}SN_3]^+$, which confirms the proposed formula. It also shows a series of peaks at 179, 168, 161, 148, 137, 121, 109, 102, 91, 76, 65 amu corresponding to various fragments (Figure 6).

The mass spectrum of the complex$[Mn(L^1)_2Cl_2]$ (1) shows a molecular ion $[M^+]$ peak at m/z 536.5 amu corresponding to the species $[Mn(C_{11}H_{15}ON_3)_2Cl_2]^+$, which confirms the proposed formula. It also shows a series of peaks at 410, 205, 175, 161, 158, 143, 132, 115, 103, 97, 91, 86, 75, 72, 61 amu corresponding to various fragments (Figure 7).

The mass spectrum of the complex$[Fe(L^1)_2Cl_2]$ (2) shows a molecular ion $[M^+]$ peak at m/z 540 amu corresponding to the species $[Fe(C_{11}H_{15}ON_3)_2Cl_2]^+$, which confirms the proposed formula. It also shows a series of peaks at 410, 205, 175, 161, 158, 143, 132, 115, 103, 97, 91, 86, 75, 72, 61 amu corresponding to various fragments (Figure 8).

The mass spectrum of the complex$[Mn(L^2)_2Cl_2]$ (3) shows a molecular ion $[M^+]$ peak at m/z 570 amu corresponding to the species $[Mn(C_{11}H_{15}SN_3)_2Cl_2]^+$, which confirms the proposed formula. It also shows a series of peaks at 440, 221, 175, 161, 158, 143, 132, 115, 103, 97, 91, 86, 75, 72, 61 amu corresponding to various fragments (Figure 9).

The mass spectrum of the complex$[Fe(L^2)_2Cl_2]$ (4) shows a molecular ion $[M^+]$ peak at m/z 571 amu corresponding to the species $[Fe(C_{11}H_{15}SN_3)_2Cl_2]^+$, which confirms the proposed formula. It also shows a series of peaks at 440, 221, 175, 161, 158, 143, 132, 115, 103, 97, 91, 86, 75, 72, 61 amu corresponding to various fragments (Figure 10).

3.7. Thermal analysis

To confirm the proposed structures for the complexes, thermogravimetric analyses TGA and DTG are measured under nitrogen. The thermal data for L^1, L^2, 1, 2, 3 and 4 are summarized in table 6. The decomposition reactions of $[Mn(L^1)_2Cl_2]$ (1) occur in four steps from 101°C to 468°C. The first step of decomposition proceeds with a weight loss of 1.85% at 101°C, associated with the loss of lattice water (calculated 1.57%). The second, third, and fourth steps of decomposition proceed at maximum temperatures of 143, 239, and 468°C, respectively, attributed to the loss of $C_{11}H_{15}ON_3$ of L_1. The total weight loss associated with these steps (72.97%) is in good agreement with the calculated value of 72.75%.
Decomposition of $[Fe(L^2)_2Cl_2)]$ (4) also occurred in four steps. Lattice water is lost at 98°C with 4.32% weight loss (calculated 4.25%). The second step of decomposition proceeded at 136°C, associated with the weight loss of 6.69% from the loss of water molecule (calculated 6.53%). The third and fourth degradation steps were observed as two consequent decomposition peaks at 238, and 467°C. The total weight loss value for the three steps was 71.74% associated with the loss of $C_{11}H_{15}SN_3$ of L_2, which agrees with the theoretical value of 71.49%.

The decomposition reactions of $[Fe(L^1)_2Cl_2)]$ (2) and $[Mn(L^2)_2Cl_2]$ (3) also occurred in four steps in a similar manner to 1 and 2 (Table 6).

3.8. Antimicrobial activity

The results of antibacterial studies were given in Table 7. Out of twelve tested organisms, the ligand L^1 shows better activity against the five gram positive bacteria such as *Staphylococcus aureus* MTCC 96, *Micrococcus luteus* MTCC 106, *Bacillus subtilis* MTCC 10619, *Bacillus cereus* MTCC 1272, *Lactobacillus* MTCC 2997 and seven gram negative bacteria such as *Salmonella typhi* MTCC 733, *Shigella flexneri* MTCC 1457, *Pseudomonas Aeruginosa* MTCC 424, *Klebsiella Pneumoniae* MTCC 7162, *Escherichia coli* MTCC 443, *Proteus vulgaris* MTCC 1771, *Proteus mirabilis* MTCC than L^2. The thiosemicarbazone metal complexes $[Mn(L^2)_2Cl_2]$ (2) and $[Fe(L^2)_2Cl_2]$ (4) show activity similar to the L^2, whereas the semicarbazone metal complexes $[Mn(L^1)_2Cl_2]$ (1), $[Fe(L^1)_2Cl_2)]$ (2) show comparatively less activity against the microbes tested.

Table 1: The numerical data of the physical measurements & CHN Elemental analysis data (in %) of L^1, L^2 and their metal complexes:

Compound	Yield	Colour	Mol. Wt.[a] (Calc.)	Melting Point (°C)	Analyses, (%) Found (Calc.)					Solubility
					C	H	N	S	M	
L^1	95%	Yellowish White	205 (205)	253	51.85 (52.14)	5.37 (5.56)	15.34 (16.76)	1.24 (0.00)	-	Ethanol, Methanol, DMSO, DMF
L^2	92%	White	221.5 (221)	223	58.88 (58.76)	6.62 (6.92)	18.75 (19.07)	13.29 (14.15)	-	Ethanol, Methanol, DMSO, DMF
$Mn(L^1)_2Cl_2$	89%	White	536.5 (536.5)	258	65.11 (66.54)	6.98 (7.02)	19.09 (19.15)	1.14 (0.00)	7.86 (7.29)	DMSO, DMF
$Fe(L^1)_2Cl_2$	75%	Dirty White	540 (537)	220	60.96 (61.08)	6.31 (6.54)	19.40 (19.76)	1.06 (0.00)	12.27 (12.62)	DMSO, DMF

$Mn(L^2)_2Cl_2$	77%	White	570 (568.5)	236	54.58 (54.97)	6.40 (6.26)	18.60 (18.75)	12.88 (13.44)	7.54 (6.58)	DMSO, DMF
$Fe(L^2)_2Cl_2$	88%	Grey	571 (569)	217	54.42 (54.32)	6.26 (6.23)	17.84 (18.31)	14.57 (14.32)	6.91 (6.82)	DMSO, DMF

[a] Molecular weights were measured using camphor as solvent

Table 2: Infra red spectral data of L^1, L^2 and their metal complexes:

Compound	ν (C=O)	ν (C=S)	ν (C=N)	ν (N-H)	ν (NH_2)	ν (M-N)	ν (M-O)	Aromatic ν (C=C)	ν (N-N)	Aromatic ν (C-H)	sp^3 C-H
L^1	1686	-	1601	3192	3459	-	-	1440	1131	3071	2956
L^2	-	1598	1590	3154	3408	-	-	1464	1282	3007	2959
$[Mn(L^1)_2Cl_2]$ (1)	1646	-	1600	3190	3459	554	607	1441	1131	3190	2956
$[Fe(L^1)_2Cl_2)]$ (2)	-	1590	1594	3156	3410	550	617	1486	1283	3008	2960
$[Mn(L^2)_2Cl_2]$ (3)	1680	-	1591	3191	3459	524	553	1440	1132	3071	2956
$[Fe(L^2)_2Cl_2)]$ (4)	-	1597	1585	3163	3415	544	620	1464	1227	3048	2957

Table 3: Electronic absorption spectral bands of L^1, L^2 and their metal complexes:

Compound	Absorption bands		
	n→π*	π→π*	d-d
L^1	30,350	39,765	
L^2	36,378	41,654	
$[Mn(L^1)_2Cl_2]$ (1)	32,986	40,033	22935, 23901, 28230

$[Fe(L^1)_2Cl_2)]$ (2)	40, 016	44,678	22935, 23901, 28230
$[Mn(L^2)_2Cl_2]$ (3)	34,587	40, 456	
$[Fe(L^2)_2Cl_2)]$ (4)	32,908	46,453	13605, 19230, 22222

Table 4: EPR g-values of metal complexes (1–4)

Compound	g-value
$[Mn(L^1)_2Cl_2]$ (1)	1.9890
$[Fe(L^1)_2Cl_2)]$ (2)	1.9965
$[Mn(L^2)_2Cl_2]$ (3)	1.9784
$[Fe(L^2)_2Cl_2)]$ (4)	1.9723

Table 5: ^{1}HNMR spectral bands of L^1, L^2 and their metal complexes:

Compound	Isopropyl CH_3 (**δ**)	Isopropyl C-H (**δ**)	Aldehydic C-H (**δ**)	NH_2 (**δ**)	NH (**δ**)	Aromatic Protons (**δ**)
L^1	1.2	3.5	10.2	6.4	2.9	7.2-7.8
L^2	1.2	3.2	10.2	6.4	2.9	7.2-8.0
$[Mn(L^1)_2Cl_2]$ (1)	1.2	3.4	10.2	6.4	2.5	7.2-7.9
$[Fe(L^1)_2Cl_2)]$ (2)	1.2	3.0	10.2	6.6	2.9	7.2-7.9
$[Mn(L^2)_2Cl_2]$ (3)	1.2	3.3	10.2	6.4	2.8	7.2-7.8
$[Fe(L^2)_2Cl_2)]$ (4)	1.2	3.0	10.1	6.5	2.9	7.2-7.9

Table 6: Maximum temperature values for decomposition along with the species lost in each step of the decomposition of the complexes

Compound	Decomposition	Tmax (°C)	Lost species	% Weight loss	
				Found	Calcd
L^1	First step	95	H_2O	2.65	2.62
	Second step	151	H_2O	5.39	5.37
	Third step	231	$C_9H_{11}O_3N_3$	75.51	75.32
	Fourth step	419		83.55	83.31
	Total loss			16.45	16.69

L^2	First step Second step Third step Fourth step Total loss	82 134 235 437	H_2O H_2O $C_9H_{11}O_2N_3S$	3.40 5.74 69.87 79.01 20.99	3.31 5.72 69.85 78.88 21.12
$[Mn(L^1)_2Cl_2]$	First step Second step Third step Fourth step Total loss Residue	101 143 239 468	H_2O Cl Cl $C_9H_{11}O_3N_3$ MnO	1.85 5.96 72.97 80.78 19.22	1.57 5.65 72.75 79.97 20.03
$[Fe(L^1)_2Cl_2]$	First step Second step Third step Fourth step Total loss Residue	93 123 245 458	H_2O Cl Cl $C_9H_{11}O_3N_3$ FeO	4.30 7.71 69.85 81.86 18.14	4.20 7.02 69.75 80.97 19.03
$[Mn(L^2)_2Cl_2]$	First step Second step Third step Fourth step Total loss Residue	105 147 246 454	H_2O Cl Cl $C_9H_{11}O_2N_3S$ MnO	2.75 5.25 74.95 82.95 17.05	2.47 4.95 74.75 82.17 17.83
$[Fe(L^2)_2Cl_2]$	First step Second step Third step Fourth step Total loss Residue	98 136 238 467	H_2O Cl Cl $C_9H_{11}O_2N_3S$ FeO	4.32 6.69 71.74 82.75 18.14	4.25 6.53 71.49 82.27 19.03

Table 7: Anti bacterial study of L^1, L^2 and their metal complexes at 0 µg/ml:

Compound	Gram Positive					Gram Negative						
	S. aureus	Mlu	B. subtilis	Bc	Lb	STM	S.flexneri	PA	KPN	E. Coli	PV	P. mirabilis
L^1	20± 1.50	17± 0.21	19± 0.65	18± 0.20	18± 1.24	19± 0.44	17± 0.98	15± 0.17	17± 0.98	18± 0.28	19± 0.65	15± 0.81
L^2	12 ± 0.89	08± 0.76	09± 1.32	05± 0.54	09± 0.76	07± 0.21	08± 0.43	07± 0.23	08± 0.43	12± 0.11	09± 1.32	07± 0.16

$Mn(L^1)_2Cl_2$	14 ± 1.01	11 ± 1.0	10 ± 0.4	07 ± 0.2	11 ± 0.6	10 ± 0.1	09 ± 0.2	08 ± 0.8	09 ± 0.2	10 ± 1.6	10 ± 0.4	11 ± 1.4 1
$Fe(L^1)_2Cl_2$	15± 0.36	13 ± 0.9	11 ± 0.2	10 ± 0.5	10 ± 0.9	10 ± 0.5	08 ± 0.2	10 ± 1.1	08 ± 0.2	12 ± 0.2	11 ± 0.2	12 ± 0.6
$Mn(L^2)_2Cl_2$	16± 0.91	10± 0.24	14± 0.11	08± 1.22	12± 0.28	14± 0.16	10± 1.10	16± 0.89	10± 1.10	10± 1.2	14± 0.11	13± 0.16
$Fe(L^2)_2Cl_2$	18 ± 0.30	13± 0.28	16± 1.06	17± 0.24	14± 0.82	15± 0.16	17± 0.28	11± 1.52	17± 0.28	18± 0.10	16± 1.06	14± 0.57

FIGURES

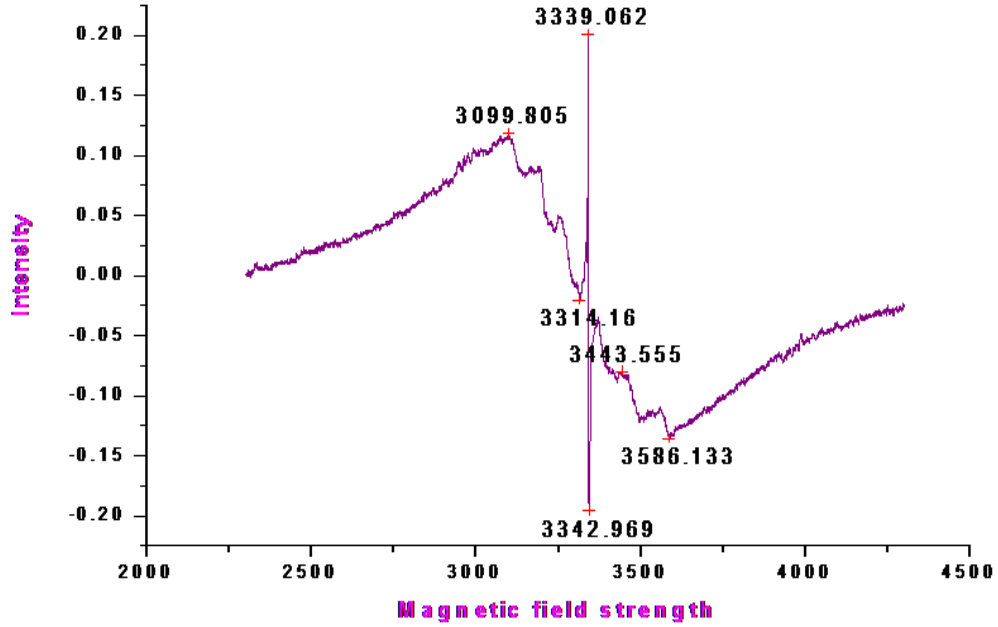

Figure 1: EPR spectrum of $[Mn(L^1)_2Cl_2]$

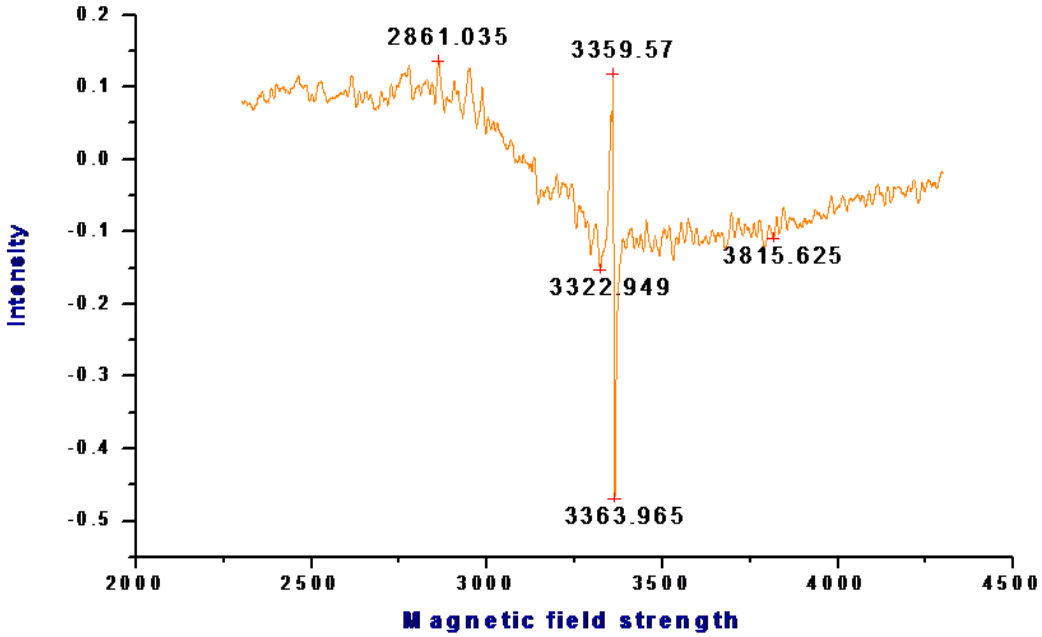

Figure 2: EPR spectrum of $[Fe(L^1)_2Cl_2]$

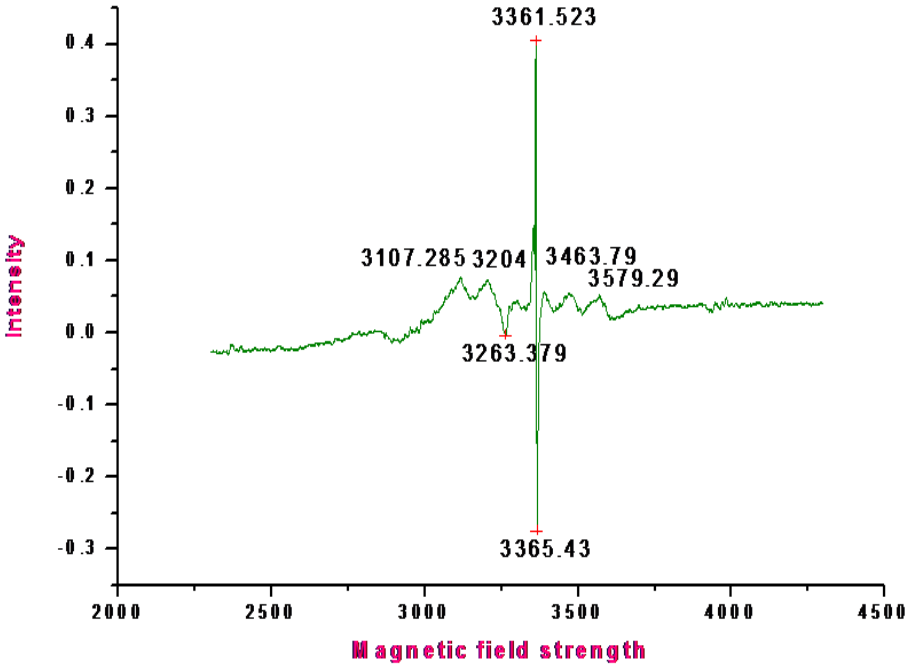

Figure 3: EPR spectrum of $[Mn(L^2)_2Cl_2]$

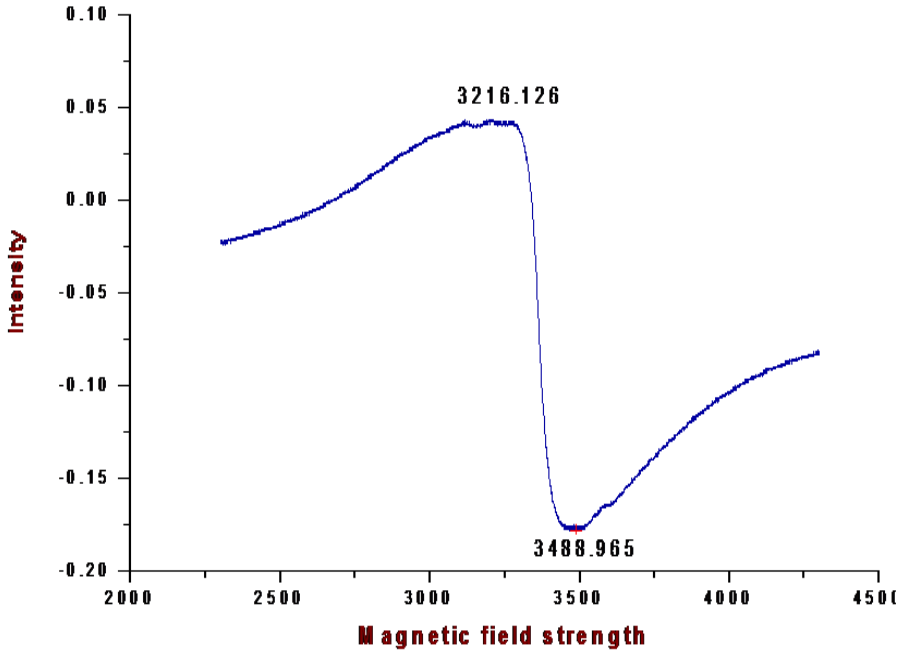

Figure 4: EPR spectrum of $[Fe(L^2)_2Cl_2]$

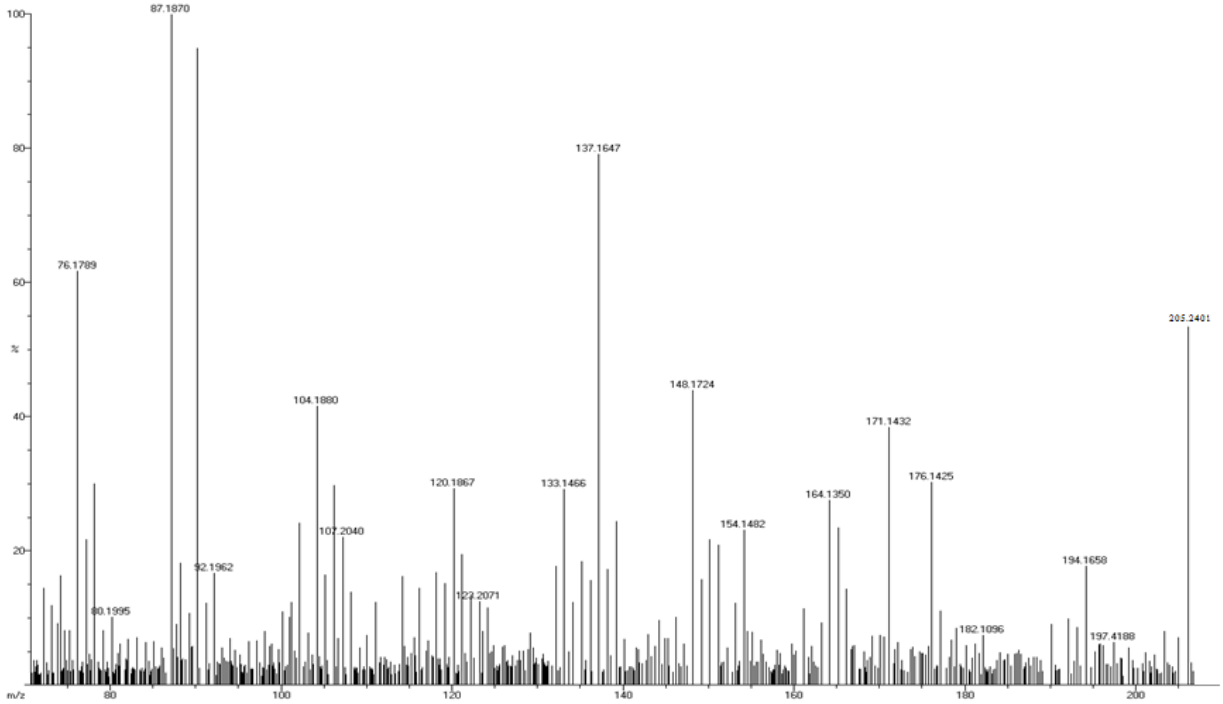

Figure 5: Mass spectrum of L^1

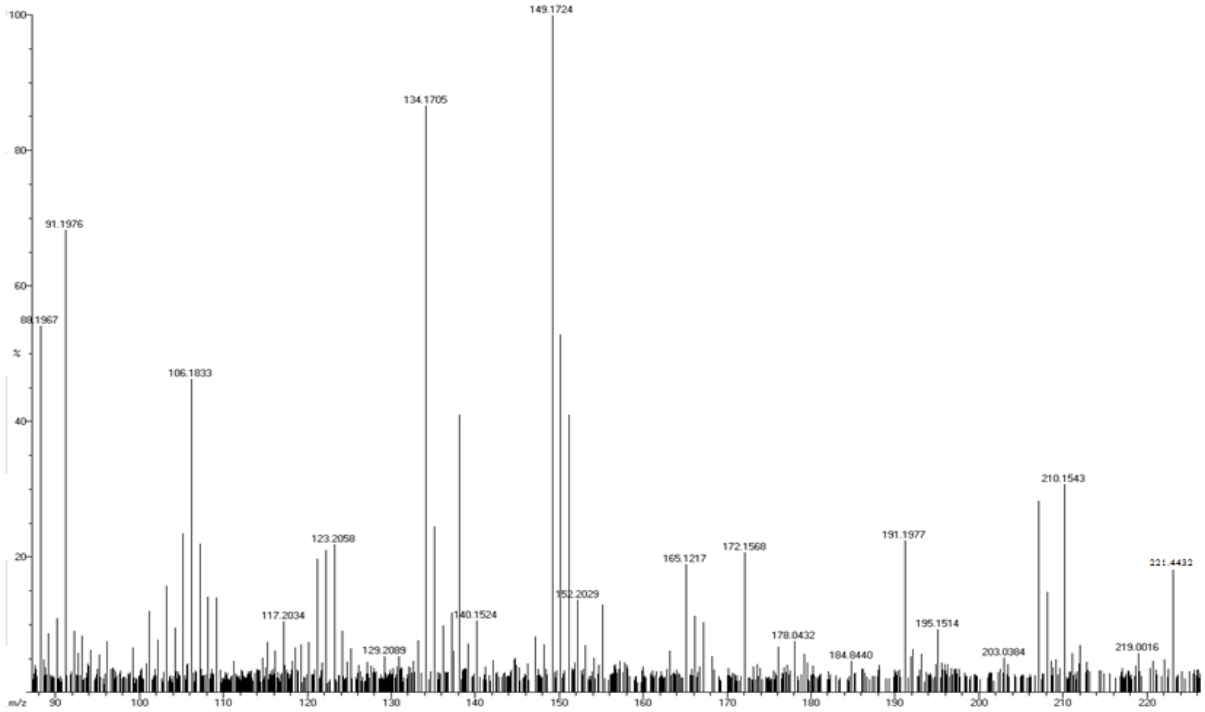

Figure 6: Mass spectrum of L^2

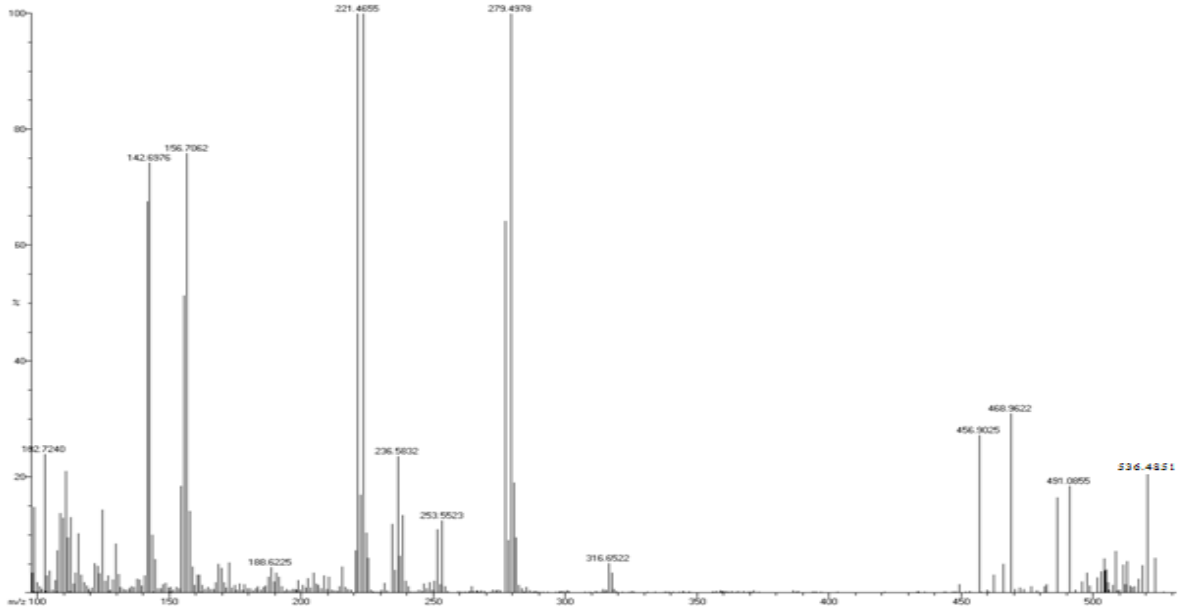

Figure 7: Mass spectrum of $[Mn(L^1)_2Cl_2]$

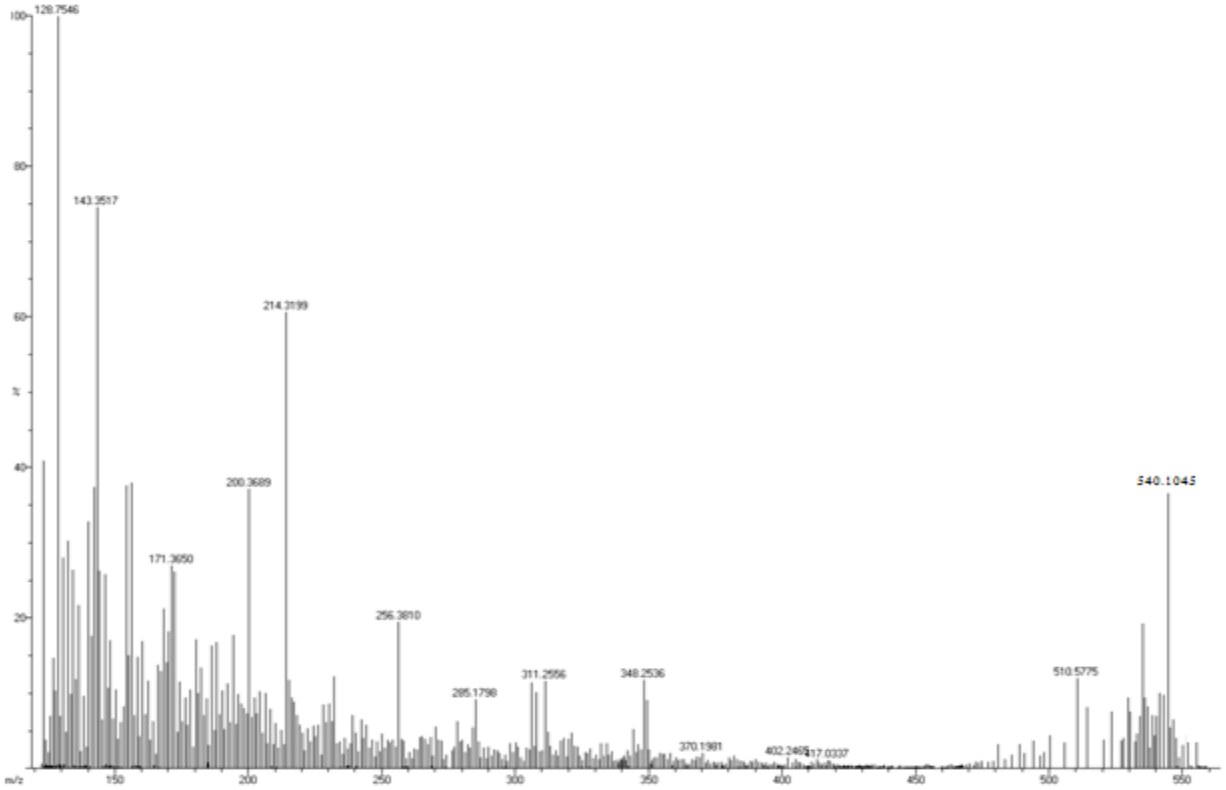

Figure 8: Mass spectrum of $[Fe(L^1)_2Cl_2]$

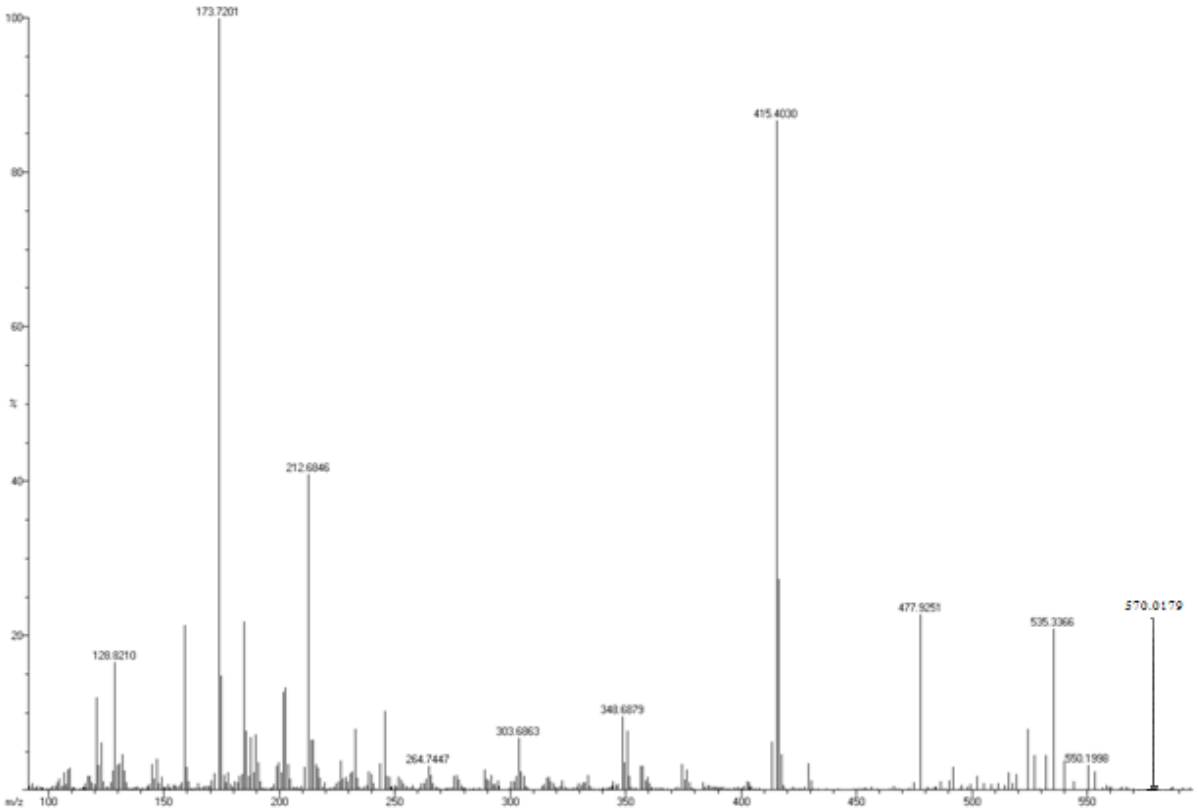

Figure 9: Mass spectrum of $[Mn(L^2)_2Cl_2]$

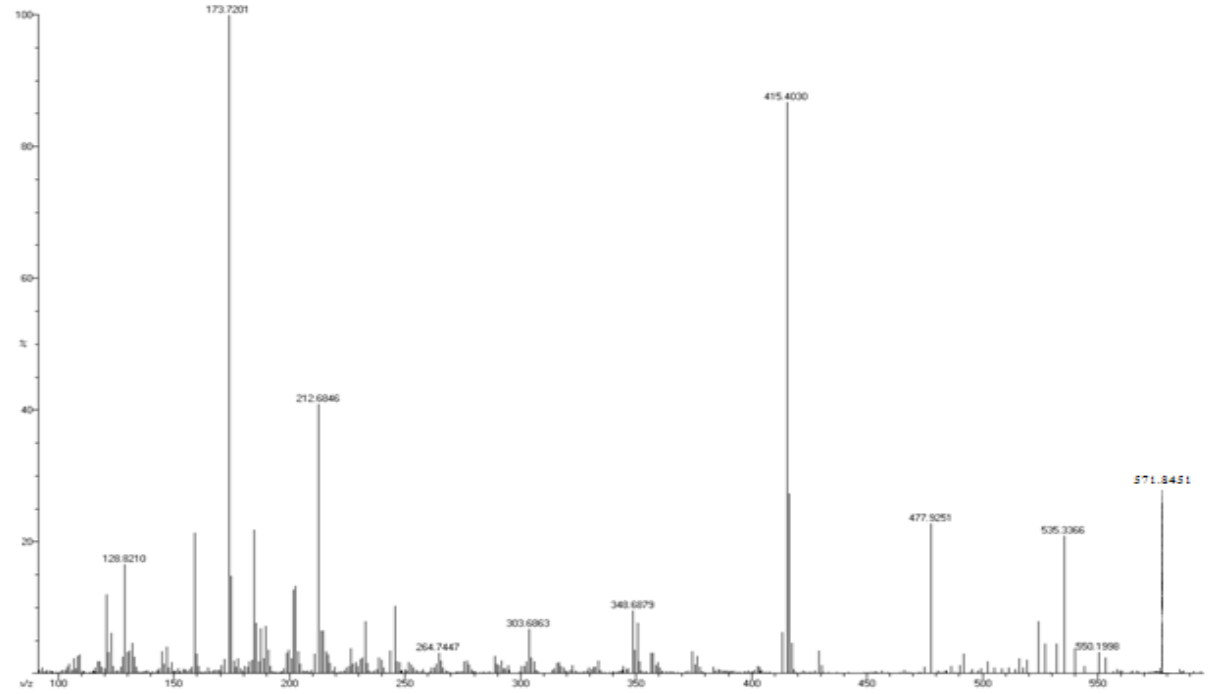

Figure 10: Mass spectrum of $[Fe(L^2)_2Cl_2]$

4. CONCLUSION

Different types of 4-isopropyl benzaldehyde semi and thiosemi carbazone metal complexes were synthesized using 4-isopropyl benzaldehyde semicarbazone / thiosemicarbazone ligands and they were characterized using IR, UV, Mass, NMR, EPR and thermal analysis. The spectral studies indicate monoanionic, bidentate nature of the ligands (L^1 and L^2), which undergo coordination to metal ions with ON or NS donor atom sets. Such metal complexation with metal/ligand stoichiometry of 1:2 leads to octahedral geometry for manganese and iron complexes.
Antibacterial studies confirmed that ligands are biologically active and their thio semicarbazone metal complexes show enhanced activity. The examined semicarbazone metal complexes show significant differences for their antimicrobial activities in comparison with the corresponding free ligand.

REFERENCES

1. N. Bharti, R.M. Maurya, F.Naqvi, A. Bhattacharya, S. Bhattacharya, A. Azam, *Eur. J. Med. Chem.* **35**, 481, (2000).
2. U. Kohn, M. Schulz, M. Gorls, E.Anders, *Tetrahedron; Asymmetry* **16**, 2125, (2005).
3. R.G.S. Berlinck, M.H. Kossuga, A. M. Nascimento, *Sci. Synth.* **18**, 1077, (2005).
4. T. Gupta, A. K. Patra, S. Dhar, M. Nethaji and A. R. Chakravarty, *J. Chem Sci.* **117**,123,(2005).
5. E. Malhotra, N.K. Kaushik, H. S. Malhotra, *Iridian J. of Chem. Sec(A),* **45A**, 370 (2006).
6. A.N.M. Kasim, D. Venkappayya, GV. Prabhu, *J. Iridian Chem. Soc.* **76**, 67, (1999).
7. N. Raman, A. Kulandaisamy, C. Thangaraja, *Transition Met. Chem.* **29**, 129, (2004).
8. F. A. Kettle, *Coordination Compounds*, (Thomas Nelson & Sons) 1975.
9. A. Gingras, R. L. Somarjai, GS. Bayley, *Can. J. Chem.*, **30**, 1865, (1968).
10. B. T Thaker, P. K. Tandel, A.S. Patel, C.J. Vyas, M.S. Jesani, D.M. Patel, *Indian J. Chem. Sec(A)* **44A**, 265, (2005).
11. B. J. Hathaway, A. A.G Tomlinson, *Coord. Chem. Rev.* **5**, 1, (1970).
12. R. Seangprasertkij, T. L. Riechel, *Inorg. Chem.* **23**, 991, (1984).
13. R. Srinivasan, I. Sougandi, R. Venkatesan, P. Sambasivarao, *Proc. Indian Acad. Sci. (Chem Sci)* **115**, 91, (2003).
14. K. Hussain Reddy, P. Sambasiva Reddy, P. Ravindra Babu, *J. Biochem.*, **11**, 169, (1999).
15. B. Macias, I. García, M.V. Villa, J. Borras, M.G. Alvarez, A. Castineiras, *J. Inorg. BioChem.* **96**, 367, (2003).
16. P. Marfey, E. Robinson, *Mutat. Res.* **86**, 1585, (1981).
17. J. C. Vincent, H.W. Vincent, *Pros. Soc. Exptl. Biol. Medi.*, **55**, 162, (1944).
18. R. S. Srivastava, *Inorg. Chim. Acta.* **56**, 65, (1944).
19. N. Gupta, R. Swaroop, R.V. Singh, *Main Group Met. Chem.* **114**, 387, (1997).
20. L. Mishra, V.K. Singh, *Iridian J. of Chem. Sec(A)* **32A**, 446,(1997).
21. R. Malhotra, S. Kumar, K.S. Dhindsa, *Indian J. Chem. Sec(A)* **32A**, 457, (1993).
22. W. Levinson, E. Jawetz, *Medical microbiology and immunology*, (4^{th} Ed., Stamford), 1996.
23. S.P. Fricker (Ed.). Metal Complexes in Cancer Therapy, Vol. 1, p. 215, Chapman and Hall, London (1994).
24. G. Berthon. Handbook of Metal–Ligand Interactions in Biological Fluids, Vol. 1 and 2, Marcel-Dekker Inc, New York (1995).
25. M.J. Clarke, P.J. Sadler (Eds.). Metallopharmaceuticals I: DNA Interactions, Vol. 1, p. 199, Springer- Verlag, Berlin (1999).
26. R.M. Roat. Bioinorganic Chemistry: A Short Course, Wiley Interscience, Hoboken, NJ (2002).
27. J.P. Kokko, J.H. Goldstein, L. Mandell. J. Am. Chem. Soc., 83, 2909 (1961).